Dual Nickel-Photoredox Catalyzed Amidine-Arylation Method Mediated By In Situ Generated Triazine Cocatalyst

Matteo Gasparetto,[1] Attila Sveiczer,[1], Andrea Fermi,[2] Mounir Raji,[1] Richard J. Fair,[3] Paola Ceroni,[2,] and Gellért Sipos[1,4,]**

[1] X-Chem Zrt., Záhony u. 7, DA Building, Graphisoft Park, 1031, Budapest, Hungary.

[2] Department of Chemistry Ciamician, University of Bologna, Via Selmi 2, 40126, Bologna, Italy.

[3] X-Chem Inc., 100 Beaver St Suite 101, Waltham, MA 02453, United States

[4] Current address: Chemaxon Kft., Váci út 133, 1138, Budapest, Hungary

**Email: Paola Ceroni paola.ceroni@unibo.it, Gellért Sipos gsipos@chemaxon.com*

Keywords: Amidine arylation, Metallaphotoredox, Flow chemistry, Reaction mechanism, Nickel catalysis

Graphical abstract

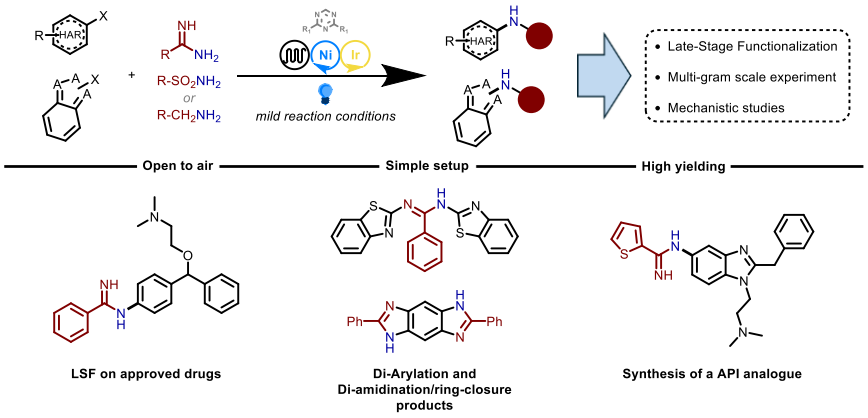

ABSTRACT

Herein, we report a high-yielding nickel/photoredox-catalyzed amidine arylation method that accommodates a wide range of aryl halides and amidines. The method exhibits good functional group tolerance enabling its successful application to both simple substrates and late-stage functionalization experiments. Mechanistic studies revealed the pivotal role of an *in situ* generated triazine co-catalyst. This information allowed us to further optimize the protocol, achieving faster reaction rates, milder conditions, and most importantly the substrate scope was expanded to sulfonamides and primary amines as well.

Introduction

Amidines, with their unique physico-chemical properties, are highly valuable compounds across diverse fields of applications, including their use as building blocks for complex molecules, organo- and transition metal catalysis, and most importantly medicinal chemistry.[1,2] Notably, amidines can serve as precursors for the synthesis of several biologically important heterocycles such as imidazoles,[3] benzimidazoles,[4,5] quinazolinones,[6,7] and quinazolines (Figure 1).[8] In recent years, compounds containing *N*-arylamidines have shown promising results in the treatment of inflammation and pain.[9]

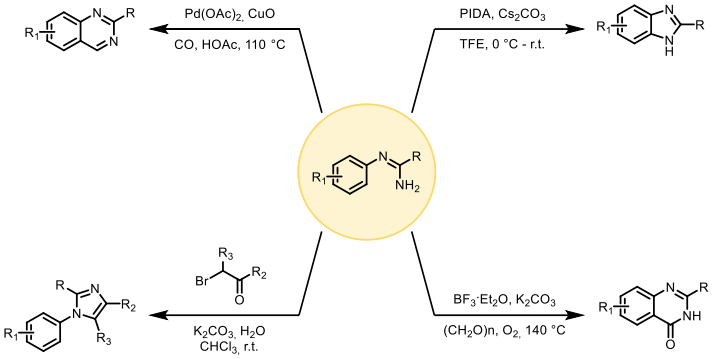

Figure 1. Synthetic versatility of *N*-aryl amidines.

Amidine derivatives are generally formed starting from the corresponding nitrile, either in a reaction with an amine using a strong base,[10–13] or through the Pinner synthesis which involves an imidate intermediate.[14–17] Both pathways require harsh conditions limiting their applicability. Direct derivatization of commercially available alkyl or aryl amidines remains a challenging transformation. In recent years, the Buchwald, Antilla, and Zhu groups tried to address this need by developing three distinct amidine arylation methods using transition metal catalysis (Figure 2A).[18–20] Despite their effectiveness, all these methods require high temperatures, long reaction times and exploit insoluble reagents limiting their applicability.

The merger of nickel and photoredox catalysis has proven to be highly effective for developing novel synthetic methodologies, including aminations,[21–23] isotopic labelling,[24,25] C-H activation,[26] and other reactions.[27–33] In particular, dual catalytic cross-coupling reactions enable milder reaction conditions compared to alternative catalytic strategies.[34–36] Specifically, nickel offers the possibility to access multiple oxidation states and a fast oxidative addition process, especially in comparison with other late transition metals, such as palladium.[37,38] The accessibility of Ni(I) and Ni(III) species makes nickel a perfect partner in metallaphotoredox reactions.[39,40] This has been demonstrated by the publication of several outstanding works where the dual-catalytic approach has been applied to perform both carbon-carbon,[41–47] and carbon-heteroatom cross-couplings (Figure 2C).[48–58] In the area of carbon–heteroatom cross-coupling, the König group reported an adaptive dynamic homogeneous procedure to obtain several connections, starting from a plethora of coupling partners (Figure 2B).[59] Amidines are briefly mentioned in König's work, but the reaction scope has not been explored. To the best of our knowledge, amidines have not been studied in detail for nickel/photoredox dual-catalytic reactions.

In this work we describe the development of a dual nickel/photoredox catalyzed amidine-arylation method compatible with a wide range of amidines, aryl and heteroaryl halides (Figure 2D). The exclusive use of liquid or soluble reagents enhances its suitability for flow chemistry applications and facilitates scale-up. We show how mechanistic investigations led to the discovery of an *in situ* generated triazine co-catalyst, and in turn to an improved synthetic protocol. The method's versatility was demonstrated through the synthesis of complex molecules, including an API derivative and late-stage functionalization steps.

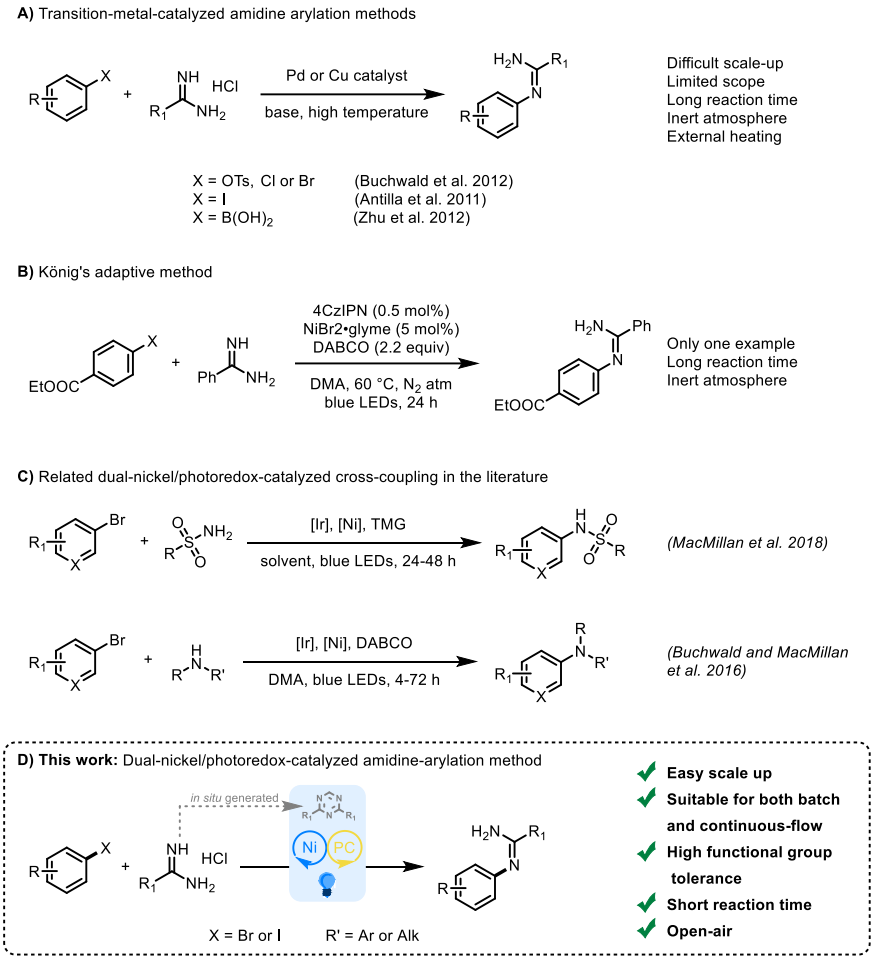

Figure 2. A) State-of-the-art transition metal-catalyzed amidine arylation methods. B) König's adaptive method for carbon-heteroatom cross-coupling. C) MacMillan's sulfonamide arylation and amine arylation methods as related Ni/hv-dual catalytic approaches. D) Our triazine-enabled Ni/*hv*-dual catalyzed amidine arylation method.

Results and discussion

Screening and optimization

We chose 4-(trifluoromethyl)picolinamidine and iodobenzene as coupling partners for preliminary optimization.[60] In line with standard conditions from the literature, our screening included solvents, photocatalysts and a pair of bases.[55,59] We decided to screen soluble components and liquid reagents to make the procedure amenable for flow chemistry applications. The plate-based evaluation allowed us to identify DBU and *fac*-Ir(ppy)$_3$ as crucial components, while both DMSO and DMF seemed to be suitable solvents (Figure 3A). To collect preliminary data on the broader applicability and the functional group tolerance of the new methodology, we evaluated a small array of aryl halides and amidines under our conditions (Supporting Information Scheme S1 and S2). We were delighted to see that the reaction proved to work with both aryl iodides and bromides, and to perform well in the presence of various functional groups.

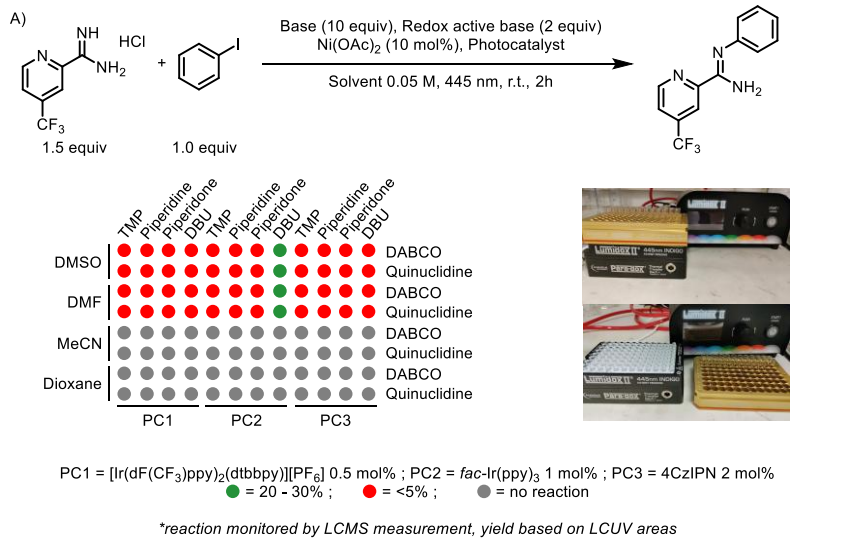

B)

HCl

DBU (10 equiv), quinuclidine (2 equiv)
Ni(OAc)$_2$ (10 mol%), Ir(ppy)$_3$ (3 mol%)
DMSO 0.05 M, 65 °C, 457 nm

1.5 equiv 1.0 equiv

Setup	Scale	Reaction time	LCMS Conversion	Isolated Yield
Batch	0.1 mmol	18 h	89%	45%
Flow	1.0 mmol	1 h	85%	54%

HCl

DBU (10 equiv), quinuclidine (2 equiv)
Ni(OAc)$_2$ (10 mol%), Ir(ppy)$_3$ (3 mol%)
DMSO 0.05 M, 65 °C, 457 nm

1.5 equiv 1.0 equiv

Setup	Scale	Reaction time	Isolated Yield
Batch	0.1 mmol	2 h	39%
Flow	1.0 mmol	1 h	38%

Figure 3. Initial screening and optimization. A) Optimization of the amidine arylation between 4-(trifluoromethyl)picolinamidine•HCl and iodobenzene using the Lumidox II photoreactor. B) Batch vs flow experiments using the PhotoCube photoreactor.

The use of flow chemistry has emerged as a very powerful tool in organic synthesis for both academic and industrial purposes.[61–64] The improved mixing and light irradiation, together with the better control over reaction conditions make flow chemistry a perfect match with photochemical methods.[45,65,66] Indeed, using continuous flow conditions we were able to reach significantly shortened reaction times on preparative scale (18 h vs 1 h, Figure 3B).

Design of Experiment is a powerful statistical tool that offers several advantages in reaction optimization in comparison to the one-factor-at-a-time approach.[67] This is particularly true for complex, multicomponent reactions, where DoE represents a fast and effective strategy for optimizing different operational and reaction conditions.[68] For this reason, we decided to perform DoE using the MODDE software which can exploit both a multi linear regression (MLR) and partial least squares regression (PLS) as statistical models to guide the optimization of the reaction parameters.[69]

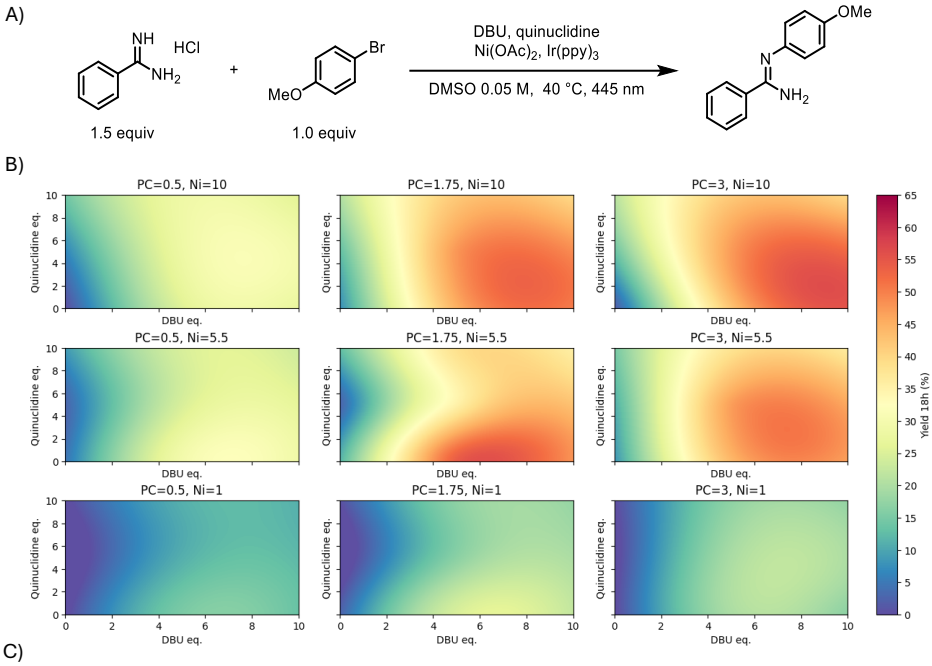

C)

Factor	Role	Value	Factor range	Factor contribution
DBU eq	Free	9.01	0.1 [■] 10	45.90
Quinuclidine eq	Free	1.09	0.1 [■] 10	0.24
PC loading	Free	1.75	0.5 [■] 3	18.39
Ni loading	Free	5.50	1 [■] 10	35.47

Figure 4. Summary of the DoE Results A) General equation of the model reaction for the DoE. B) Response contour of LCMS yields after 18 h (PLS). PC refers to $Ir(ppy)_3$ photocatalyst (mol%), Ni refers to $Ni(OAc)_2$ (mol%). C) Predicted optimal conditions and factor contributions in percentage.

In this context, we moved to the investigation of the coupling reaction between a simple amidine and a more challenging aryl halide, selecting benzamidine and 4-bromoanisole as the model for our DoE (Figure 4) and the following control experiments (Table 1). The inputs for the optimization consisted of four continuous factors, representing the amounts of different reagents, while the LCMS yields at 2, 5, and 18 hours served as the measurable outputs to be optimized. A total of 27 batch experiments were conducted, and the data were analyzed using different statistical models to predict the optimal experimental conditions and maximize product yield at 18 h. The results showed that nickel, photocatalyst and DBU are important contributors to the outcome. More detailed information on the DoE analysis can be found in the Supporting Information.

Control experiments confirmed that the reaction is both nickel- and photo-catalyzed, as no product formation was observed without nickel acetate, photocatalyst or light irradiation, even under heating (Table 1, Entries 2, 6-8). Since $Ir(ppy)_3$ has an absorption maximum at 377 nm in DMSO (Supporting Information, Figure S12), we tested the reaction using a 390 nm light source (Table 1, Entry 11). Surprisingly, the reaction failed entirely under purple light irradiation. This result can indicate the presence of unfavorable optical effects (inner filter effects). The condition predicted by the software after the DoE, [69,70] proved to be the best both in terms of outcome and reaction rate (Table 1, Entry 12). The optimized conditions were tested both with nickel acetate and with commercially available nickel complex $(dtbbpy)NiCl_2$. The reaction worked well in both cases, but the use of the nickel bipyridyl complex led to lower reaction rate. However, while DBU seemed crucial to reach full conversion, quinuclidine didn't seem to have the same importance for the reaction outcome, as also indicated by the DoE analysis, therefore it was not used in following parts of the study.

Table 1. Control experiments on the amidine arylation reaction between benzamidine and 4-bromoanisole.

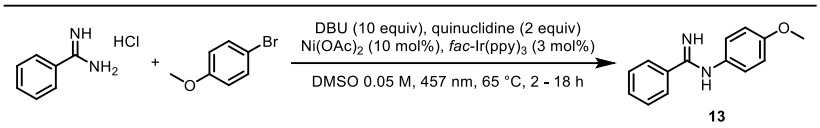

13

Entry	Deviation	LCUV Conversion		
		2 h	5 h	18 h
1	None	39%	69%	97%
2	No nickel	---	---	---
3	No DBU (2 equiv quinuclidine)	12%	14%	25%
4	No DBU (10 equiv quinuclidine)	60%	70%	85%
5	No quinuclidine	59%	80%	98%
6	No photocatalyst	---	---	---
7	No light	---	---	---
8	No light (65 °C)	---	---	---
9	MeCN instead of DMSO	---	---	---
10	45 °C instead of 65 °C	24%	53%	91%
11	390 nm instead of 457 nm	---	---	---
12	**2 mol% [Ir], 5.5 mol% $Ni(OAc)_2$, 9 equiv DBU and 1.1 equiv quinuclidine (DoE Conditions)**	**62%**	**84%**	**100%**
13	DoE conditions with 5.5 mol% $(dtbbpy)NiCl_2$ instead of $Ni(OAc)_2$	50%	71%	96%

Scope investigation and applications

With the optimized conditions in hand, we sought to examine the generality of our transformation (Figure 5). A variety of aryl halides bearing both electron-withdrawing (EWG) as well as electron-donating groups (EDG) proved to be amenable to the continuous flow reaction protocol, leading to the arylated amidines **1 - 18** in good to excellent yield (59 to 99%). Substrates featuring strong EWGs gave excellent yields (99% for **2** and **3**). Ambivalent compounds in which the electron-withdrawing inductive effect combines with an electron donating resonance contribution, are working nicely in our conditions (81-93% for **4-8**). Notably, the synthesis of compound **6** was performed with just 1.1 equiv of coupling partner (vs 1.5 equiv. for the other substrates) to avoid double amidination. Generally speaking, EDGs seem to be well tolerated as well (80-99% for **9**, **11**-**13**), only compound **14** featuring the strong electron-donating p-$N(Me)_2$ group afforded moderate yield (59%). Reaction with meta functionalized aryl halides proceeded smoothly (88-99% for **10**, **15**-**18**). Unfortunately, except for 1-fluoro-2-iodobenzene (affording substrate **8** in 91% yield), ortho-substituted aryl halides are not compatible with our reaction conditions. Even though ortho-substituted aryl halides are typically challenging coupling partners in similar cross coupling reactions, the complete halt of the reaction is still surprising.[28,71–73]

Our protocol proved to work well also with a variety of heteroaryl halides. Halopyridines are reactive partners in our conditions, leading to the formation of compounds **19** and **20** in 77% and 25% yield, respectively. The low yield for compound **20** is due to the excessive reactivity of 2-iodopyridine, which led to the formation of di- and tri-arylated benzamidine by-products, despite benzamidine being used in excess. 3-Bromoquinoline proved to be a challenging substrate in this coupling reaction due to the presence of a competing dehalogenation pathway which decreased the yield for compound **21** to 39% in flow and 45% in batch conditions. The procedure proved to work even with challenging substrates like 5-iodopyrimidine and 2-bromobenzo[*d*]thiazole leading to compounds **22** and **28** in 35% and 70% yield, respectively. 2-Iodopyrimidine proved to be amenable to our transformation, as well as indoles, indazoles and benzimidazoles derivatives, leading to compounds **23 – 27** in excellent yields. Both aryl iodides and bromides can be subjected to the amidination reaction (e.g. **1**, **3**, **13**), however, aryl chlorides do not react under these conditions.

An array of amidines were tested to explore their compatibility as coupling partners. The reaction performed well with aryl amidines (**29** to **31**), benzyl amidine (**32**), heteroaryl amidines (**34** to **36**), and alkyl amidines (**37** and **38**). All the tested compounds led to product formation in good to excellent yields, although picolinamidines and alkyl amidines proved to be more difficult coupling partners. In contrast to aryl halides, ortho substitution is tolerated on the amidines (**31**). We tested the protocol on different classes of coupling partners, such as amines and sulfonamides but unfortunately, those substrates do not react under the conditions shown in Figure 5.

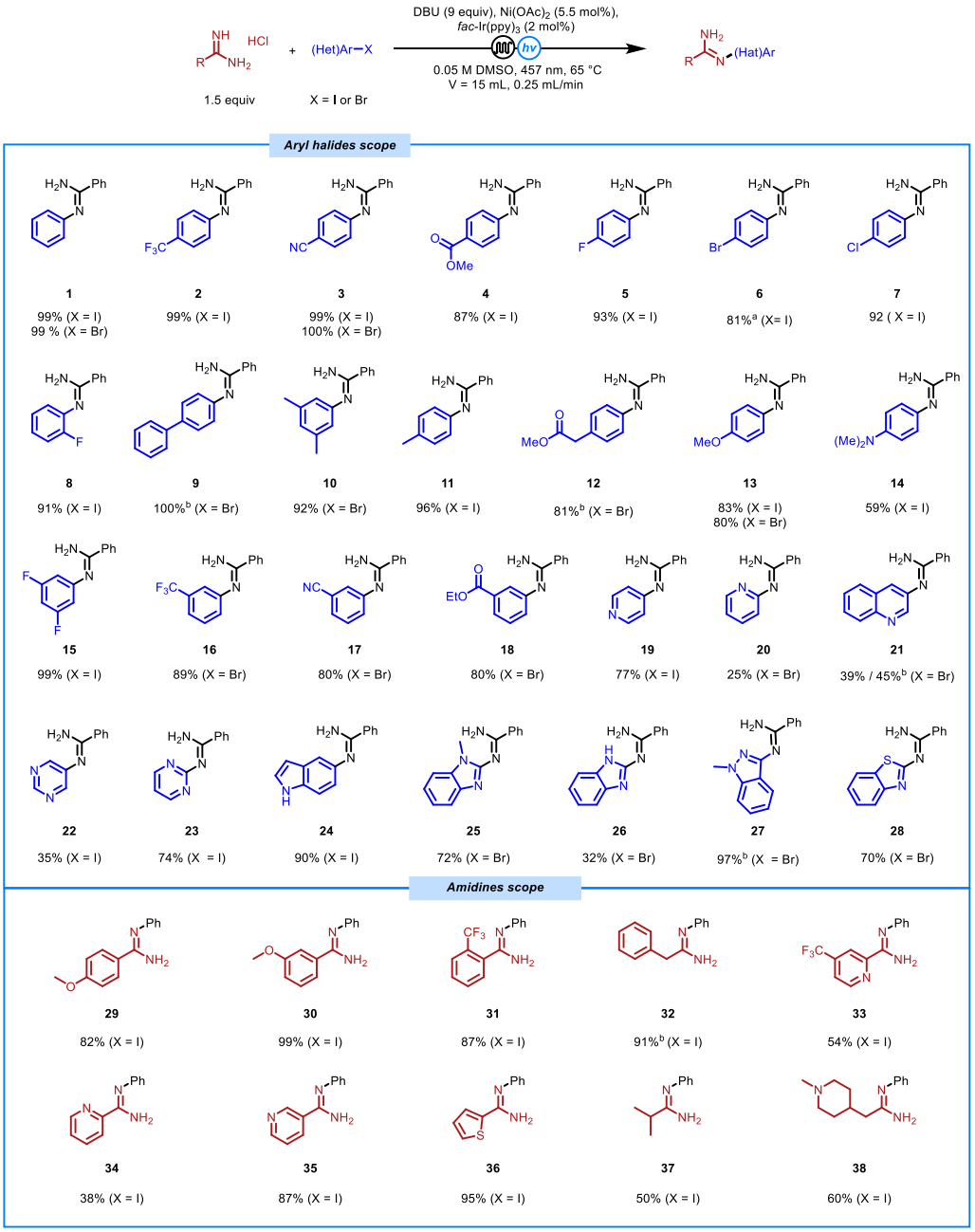

Figure 5. Substrate scope. All reactions were performed under continuous flow conditions in the PhotoCube™ reactor. Isolated yields are reported. In brackets is reported which haloaryl was used for the reaction. (a) **amidine** (1.1 equiv). (b) **batch conditions** 2-16 h (reaction time reported in the Supporting information).

To further evaluate the robustness and applicability of our protocol, we extended its use to the synthesis of complex molecules and late-stage functionalization (LSF) experiments on bioactive compounds (Figure 6). The procedure was adapted for a diamidination protocol using benzamidine with both 1,4-diiodobenzene and 1,4-dibromobenzene, leading to compound **39** in good yields (70% and 59%, respectively). This intermediate was then subjected to double ring-closure affording UV-protecting agent **41** in moderate yield (Figure 6A).[74] We also attempted di-arylation of benzamidine using 2-bromobenzothiazole as the arylating agent, obtaining compound **40** in 40% isolated yield (Figure 6B). In addition, when the anti-histaminic drug bromazine (**43**) was subjected to our amidination protocol **44** was obtained in excellent yield (Figure 6C). We found a reported nNOS inhibitor with μ-opioid agonist activity, [9] where

our amidine arylation method can be utilized. Finally, we designed a route where, by applying our method twice, we were able to synthesize a closely related analogue (**48**) in only four steps (Figure 6D).

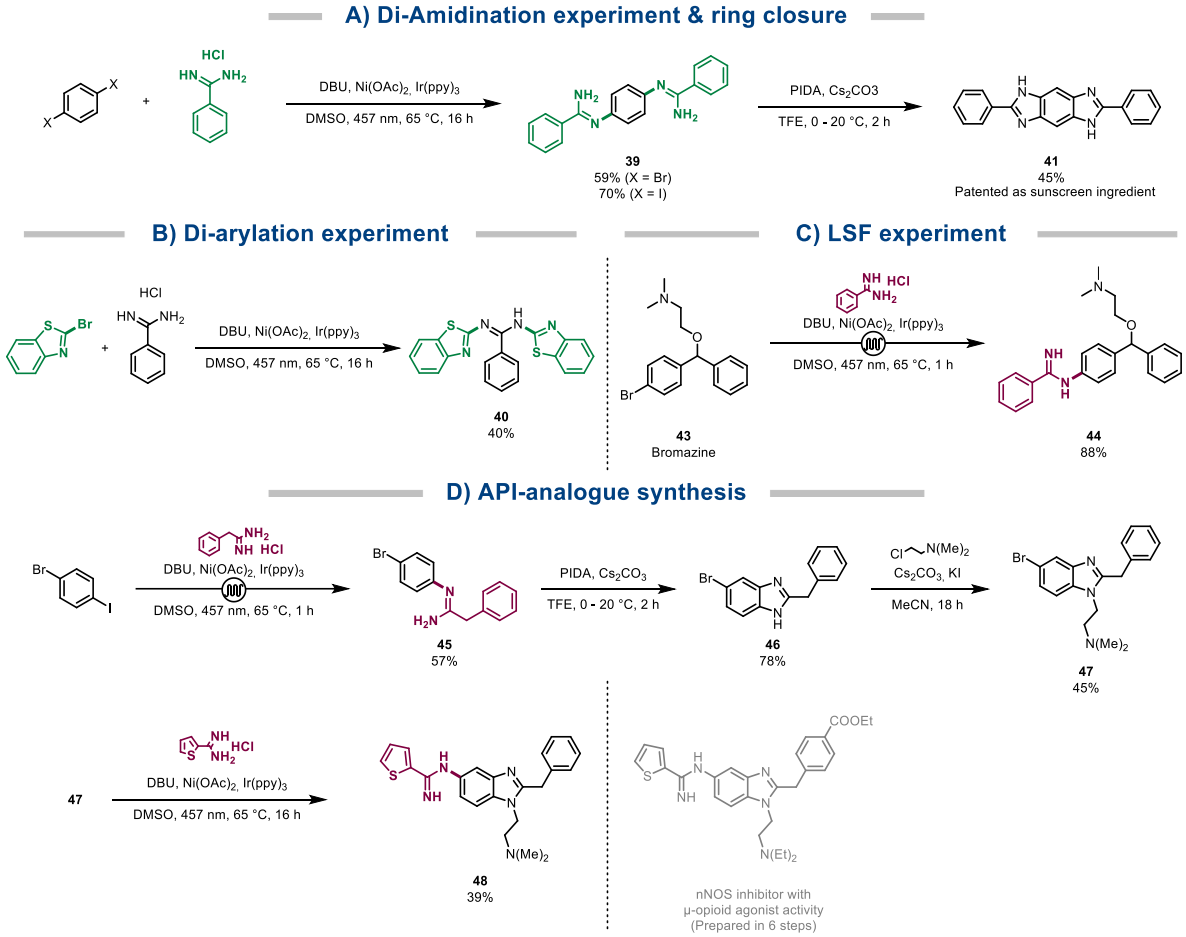

Figure 6. Diversification, late-stage functionalization and API-analogue synthesis. All yields are for isolated compounds. Detailed procedures and conditions are reported in the Supporting information.

Mechanistic investigation

To gain deeper insights into this transformation, a series of control experiments was designed, using the coupling between iodobenzene and benzamidine as the model reaction. Combining spectroscopic and experimental data, we ruled out the possibility of an energy transfer (EnT) mechanism for our methodology.[75] Preliminary experiments showed how the reaction is completely inhibited if a radical scavenger like TEMPO or 4-hydroxy-TEMPO is added to the mixture, indicating the formation of an organic radical species in the reaction pathway (Figure 7A, entries 3 and 4).

The possibility of a single-electron transfer (SET) mechanism was explored through time-correlated single-photon counting (TCSPC) experiments to identify the quencher of the photocatalyst's excited state. From an initial screening, none of the individual reaction components was found to quench the excited state of $Ir(ppy)_3$. TCSPC analysis of the complete reaction mixture revealed no decrease in the emission lifetime decay of the photocatalyst, thus an experiment under deoxygenated conditions was conducted to assess a potential effect of

oxygen species. The reaction proceeded efficiently even without oxygen, ruling out its involvement in the mechanism (Figure 7A, entry 2).[76] At this point, we hypothesized that a new species might have been forming *in situ* during the initial minutes of irradiation. To confirm this assumption, first the reaction mixture (without the photocatalyst) was irradiated under 390 nm light for 3 hours. Next, the *a priori* irradiated mixture was used in a TCSPC experiment resulting in significant quenching of the phosphorescent excited state of $Ir(ppy)_3$. Benzamidine proved to be a crucial component for the formation of the quencher, and literature analysis indicated the potential formation of a triazine derivative under reaction conditions (Figure 7B).[77] Indeed, independently prepared 2,4-diphenyl-1,3,5-triazine (**49**) proved to be a good quencher of the lowest excited state of $Ir(ppy)_3$ (Figure 7C, see SI for details).

Cyclic voltammetry studies show that formation of triazine radical anion **49**$^{\bullet-}$ is energetically favored (reductive potentials of -1.77 V vs SCE for Ir^{IV}/$*Ir^{III}$ and -1.67 V vs SCE for **49**/**49**$^{\bullet-}$ were estimated).

A reaction conducted in presence of **49**, but without the amidine starting material resulted in the formation of dehalogenation and homocoupling side products. These finding indicate that triazine radical anion might play a role in the reduction of Ni(II) to Ni(I), which can then readily undergo an oxidative addition process with the aryl halide as confirmed by cyclic voltammetry study (Figure 7D). The radical reduction of the nickel species is supported electrochemically, with a measured $E_{1/2}$ value for Ni^{II}/Ni^{I} of -1.57 V vs SCE (vs the -1.67 V vs SCE for **49**/**49**$^{\bullet-}$).

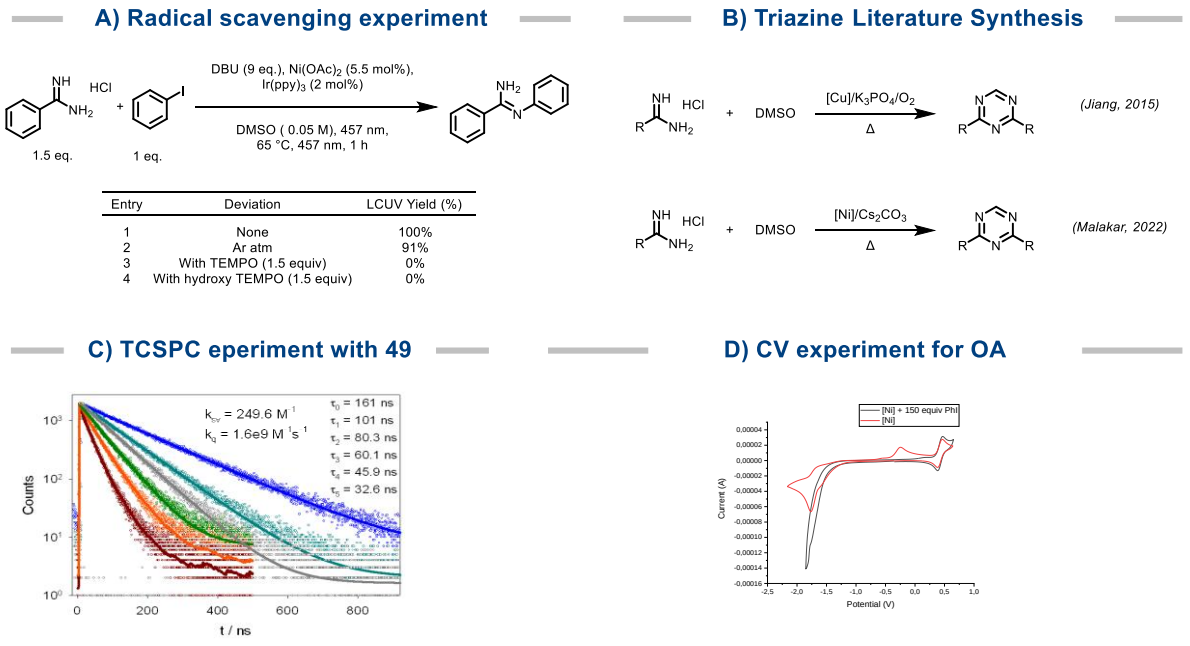

Figure 7. A) Radical scavenging experiments and the effect of oxygen. B) Literature protocols for the synthesis of substituted triazines from amidines. C) Quenching of the excited state of $Ir(ppy)_3$ in aerated DMSO with increasing amount of 2,4-diphenyl-1,3,5-triazine (**49**). D) Cyclic voltammetry study for oxidative addition (OA). Oxidative addition study: $Ni(OAc)_2$ and 150 equiv of iodobenzene. [Ni] = 2 mM in DMSO; [TEAP] = 200 mM in DMSO; Scan rate: 0,1 V/s; WE: Glassy carbon; CE: Pt; RE: Ag.

Based on the above findings and the precedents in the literature we propose the following reaction mechanism for the Ir/Ni dual-catalyzed amidine arylation method (Figure 8).[78–81] The heat generated upon irradiation and light absorption, initiates the nickel-catalyzed formation of the co-catalyst **49** (Figure 8A). Once the triazine is formed, it efficiently quenches the excited-state photocatalyst via a single-electron transfer, yielding Ir(IV) and the triazine radical anion (**49**·⁻). The radical subsequently reduces Ni(II) to Ni(I), which undergoes oxidative addition onto the aryl halide to form the Ni(III) complex **I**. Ligand exchange then produces key intermediate **II**, which, due to its higher oxidation state relative to the more stable Ni(II), undergoes rapid reductive elimination. This step generates the desired product while regenerating Ni(I). Photocatalyst turnover is most plausibly achieved through a back-electron transfer between the triazine radical anion and Ir(IV), similarly to the mechanism reported by MacMillan in 2020.[80]

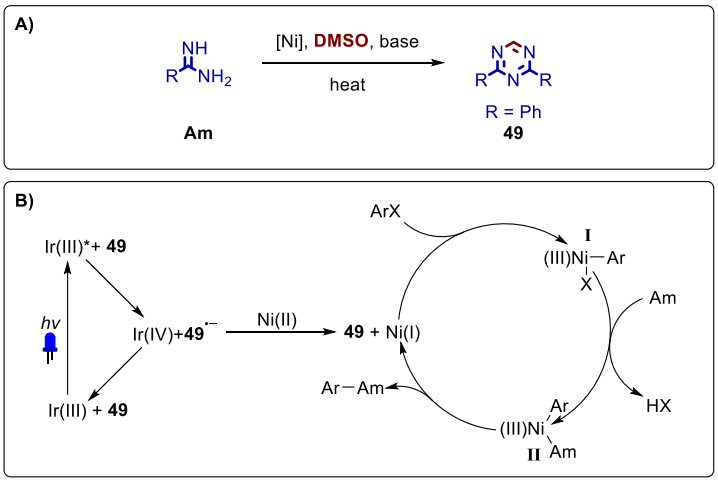

Figure 8. A) General equation for the *in situ* formation of the triazine co-catalyst (**49**). B) Plausible mechanism for the nickel-photoredox dual catalyzed amidine-arylation.

In order to confirm our proposed mechanism a series of experiments were designed to elucidate the effect of the addition of **49** to the initial reaction mixture (Table 2). Product formation proceeded rapidly in the presence of **49**, affording complete conversion within 15 minutes (Table 2 Entries 1 and 2). An on-off experiment confirmed that the nickel cycle does not sustain itself without irradiation, instead it deactivates rapidly (see SI).[80] Photocatalyst, light, nickel(II) acetate and DBU are all vital for the reaction to proceed (Table 2 Entries 3-6). Since heat, large amount of base, and DMSO are no longer required to form **49**, the reaction proceeded efficiently in different solvents and under milder reaction conditions (Table 2 Entries 7-10).

Table 2. Control experiments for the improved protocol

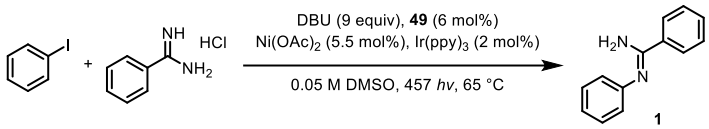

Entry	Deviation	LCUV Yield (%)	
		15 min	1 h
1	None	100	100
2	No **49**	16	100
3	No PC	0	0
4	No light	0	0
5	No $Ni(OAc)_2$	0	0
6	No DBU	0	0
7	1.5 equiv DBU	95	100
8	40 °C	100	100
9	MeCN instead of DMSO	82	100
10	DMA instead of DMSO	100	100

*Improved synthetic method with 2,4-diphenyl-1,3,5-triazine (**49**)*

Discovering the role of the triazine species led us to explore the synthetic utility of the new catalytic system. Addition of the triazine co-catalyst **49** to the reaction mixture led to faster reaction time (15 min vs 60 min), and to a productivity increase from 0.19 g/h to 0.84 g/h in our flow system (Table 3A). Scaling up the reaction to 11 mmol went without an issue, affording 2.1 g of **1** in only 2.5 h process time (Table 3B).

Sulfonamides and amines did not perform under the original methodology. Employing **49** allowed us to include them in the scope of the reaction. While sulfonamides provided high yields, benzylamine and other amines produced side products and showed lower yields when $Ni(OAc)_2$ was used (Table 3C, top row). The initial control experiments highlighted that using (dtbbpy)$NiCl_2$ resulted in a slower reaction rate (Table 1, Entry 13), which in some cases might favor the formation of the desired compound over side reactions. A quenching study indicated that this nickel complex can act as a quencher for the photocatalyst, although it exhibits a smaller quenching constant in comparison with **49** (Supporting Information Figure S28), explaining the lower reaction rate. Armed with these insights, we tested sulfonamides and amines using (dtbbpy)$NiCl_2$ as both nickel source and quencher, achieving high yields for both, albeit with reduced reaction rate and productivity over time (Table 3C, bottom row). It should be noted that the conditions featuring (dtbbpy)$NiCl_2$ are similar to those developed by Escobar and Johannes, therefore it is safe to assume that the reaction follows a different mechanism.[82]

Finally, this improved method was successfully tested on the slow reacting substrate **13** which required 18 h to obtain 80% isolated yield (batch reaction, Table 3D top). The addition of **49** allowed us to obtain the desired product in comparable yield in just 5 h in batch and within 2.5 h in flow, using milder conditions and a significantly reduced base loading (2 equiv. instead of 9) (Table 3D, bottom).

Table 3. Improved method

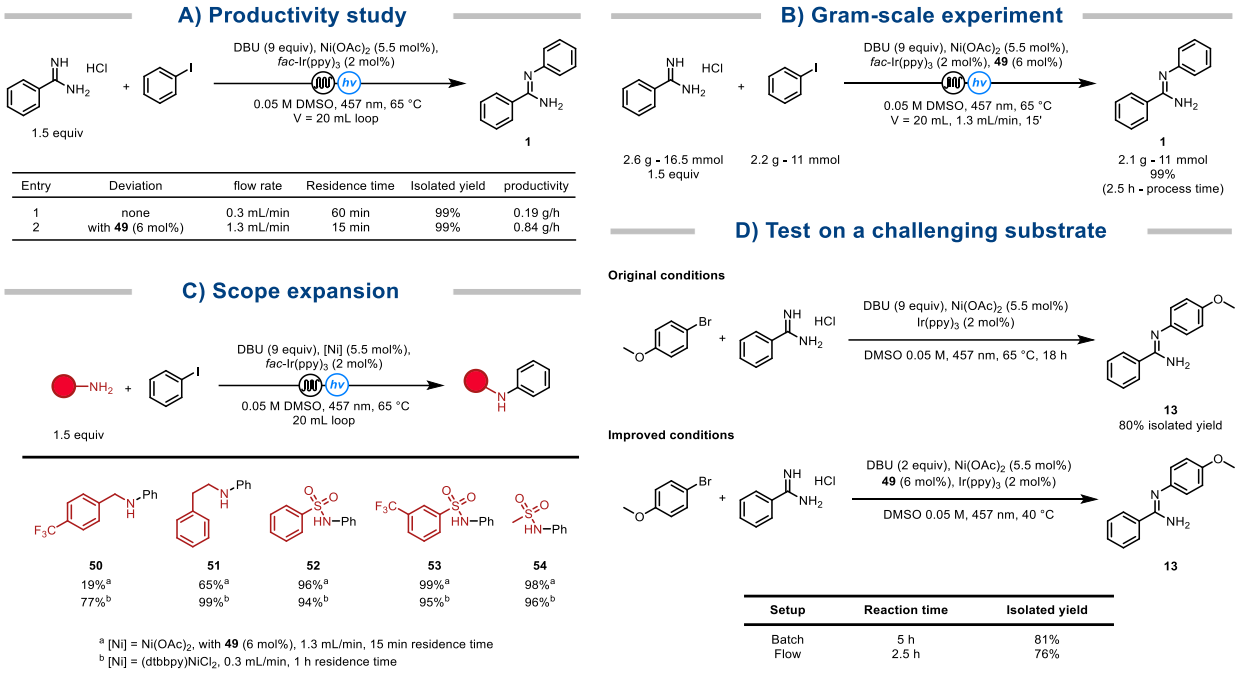

Entry	Deviation	flow rate	Residence time	Isolated yield	productivity
1	none	0.3 mL/min	60 min	99%	0.19 g/h
2	with **49** (6 mol%)	1.3 mL/min	15 min	99%	0.84 g/h

[a] [Ni] = $Ni(OAc)_2$, with **49** (6 mol%), 1.3 mL/min, 15 min residence time
[b] [Ni] = $(dtbbpy)NiCl_2$, 0.3 mL/min, 1 h residence time

Conclusions

In conclusion, we have developed a practical, high-yielding amidine arylation method in continuous flow that operates in open-air, under mild conditions. A plethora of (hetero)aryl halides and amidines are amenable to our protocol which has also been successfully applied in a late-stage functionalization and in the synthesis of biologically relevant molecules. Mechanistic studies revealed how an *in situ* generated triazine co-catalyst plays a critical role in achieving productive transformation. These learnings allowed us to not only increase the productivity of the synthetic methodology, but to also expand the scope to include sulfonamides and primary amines.

Acknowledgements

M.G., P.C. and G.S. thank the European Union for funding under the PhotoReAct Project, H2020 Marie Sklodowska-Curie grant agreement No.956324 (MSCAITN: PhotoReAct). M.G. thanks the Ceroni group and the whole Chemistry Department Giacomo Ciamician at University of Bologna for hosting him and supporting him during the mechanistic investigation studies. The authors thank Dr. Ying Zhang and Dr. Anthony D. Keefe for proofreading this manuscript.

Conflict of Interest

The authors declare no conflict of interest.

Data Availability Statement

The data that support the findings of this study are available in the supplementary material of this article.

References

[1] A. A. Aly, A. M. Nour-El-Din, *Arkivoc* **2008**, 153–194.

[2] A. A. Aly, S. Bräse, M. A. M. Gomaa, *Arkivoc* **2018**, *2018*, 85–138.

[3] T. Wiglenda, I. Ott, B. Kircher, P. Schumacher, D. Schuster, T. Langer, R. Gust, *J. Med. Chem.* **2005**, *48*, 6516–6521.

[4] G. Brasche, S. L. Buchwald, *Angew. Chem. Int. Ed.* **2008**, *47*, 1932–1934.

[5] J. Huang, Y. He, Y. Wang, Q. Zhu, *Chem. Eur. J.* **2012**, *18*, 13964–13967.

[6] B. Ma, Y. Wang, J. Peng, Q. Zhu, *J. Org. Chem.* **2011**, *76*, 6362–6366.

[7] Z. S. Sales, N. S. Mani, B. D. Allison, *Tetrahedron Lett.* **2018**, *59*, 1623–1626.

[8] X. Cheng, H. Wang, F. Xiao, G. J. Deng, *Green Chem.* **2016**, *18*, 5773–5776.

[9] P. Renton, B. Green, S. Maddaford, S. Rakhit, J. S. Andrews, *ACS Med. Chem. Lett.* **2012**, *3*, 227–231.

[10] L. Song, X. Tian, Z. Lv, E. Li, J. Wu, Y. Liu, W. Yu, J. Chang, *J. Org. Chem.* **2015**, *80*, 7219–7225.

[11] E. P. Arnold, P. K. Mondal, D. C. Schmitt, *ACS Comb. Sci.* **2020**, *22*, 1–5.

[12] Q. Xiao, W. H. Wang, G. Liu, F. K. Meng, J. H. Chen, Z. Yang, Z. J. Shi, *Chem. Eur. J.* **2009**, *15*, 7292–7296.

[13] Y. Wang, H. Wang, J. Peng, Q. Zhu, *Org. Lett.* **2011**, *13*, 4604–4607.

[14] K. Schärer, M. Morgenthaler, R. Paulini, U. Obst-Sander, D. W. Banner, D. Schlatter, J. Benz, M. Stihle, F. Diederich, *Angew. Chem. Int. Ed.* **2005**, *44*, 4400–4404.

[15] T. R. M. Rauws, B. U. W. Maes, *Chem. Soc. Rev.* **2012**, *41*, 2463–2497.

[16] T. Brückl, F. Klepper, K. Gutsmiedl, T. Carell, *Org. Biomol. Chem.* **2007**, *5*, 3821–3825.

[17] S. Caron, L. Wei, J. Douville, A. Ghosh, *J. Org. Chem.* **2010**, *75*, 945–947.

[18] M. A. McGowan, C. Z. McAvoy, S. L. Buchwald, *Org. Lett.* **2012**, *14*, 3800–3803.

[19] J. Li, S. Bénard, L. Neuville, J. Zhu, *Org. Lett.* **2012**, *14*, 5980–5983.

[20] M. Cortes-Salva, C. Garvin, J. C. Antilla, *J. Org. Chem.* **2011**, *76*, 1456–1459.

[21] R. A. Green, J. F. Hartwig, *Angew. Chem. Int. Ed.* **2015**, *54*, 3768–3772.

[22] S. Ge, R. A. Green, J. F. Hartwig, *J. Am. Chem. Soc.* **2014**, *136*, 1617–1627.

[23] J. P. Wolfe, S. L. Buchwald, *J. Am. Chem. Soc.* **1995**, *34*, 6054–6058.

[24] F. Minya, Á. Mészáros, E. Csizmadia, D. Suskó, M. Raji, G. Sipos, *Adv. Synth. Catal.* **2025**, 367, e202400168.

[25] N. Pootheri, S. Lee, *Adv. Synth. Catal.* **2023**, *365*, 3950–3957.

[26] J. Loup, V. Müller, D. Ghorai, L. Ackermann, *Angew. Chem. Int. Ed.* **2019**, *58*, 1749-1753.

[27] I. Koyama, T. Kurahashi, S. Matsubara, *J. Am. Chem. Soc.* **2009**, *131*, 1350–1351.

[28] X. Du, I. Cheng-Sánchez, C. Nevado, *J. Am. Chem. Soc.* **2023**, *145*, 12532–12540.

[29] L. Liu, C. Nevado, *Organometallics* **2021**, *40*, 2188–2193.

[30] C. Zhu, H. Yue, L. Chu, M. Rueping, *Chem. Sci.* **2020**, *11*, 4051–4064.

[31] F. Calogero, S. Potenti, E. Bassan, A. Fermi, A. Gualandi, J. Monaldi, B. Dereli, B. Maity, L. Cavallo, P. Ceroni, P. G. Cozzi, *Angew. Chem. Int. Ed.* **2022**, *61*, e202114981.

[32] F. Calogero, G. Magagnano, S. Potenti, A. Gualandi, A. Fermi, P. Ceroni, P. Giorgio Cozzi, *Adv. Synth. Catal.* **2022**, *364*, 3410–3419.

[33] A. Gualandi, G. Rodeghiero, A. Faraone, F. Patuzzo, M. Marchini, F. Calogero, R. Perciaccante, T. P. Jansen, P. Ceroni, P. G. Cozzi, *Chem. Comm.* **2019**, *55*, 6838–6841.

[34] C. Zhu, H. Yue, J. Jia, M. Rueping, *Angew. Chem. Int. Ed.* **2021**, *60*, 17810–17831.

[35] W. Xu, T. Xu, *Acc. Chem. Res.* **2024**, *57*, 1997–2011.

[36] M. D. Palkowitz, M. A. Emmanuel, M. S. Oderinde, *Acc. Chem. Res.* **2023**, *56*, 2851–2865.

[37] S. Z. Tasker, E. A. Standley, T. F. Jamison, *Nature* **2014**, *509*, 299–309.

[38] P. P. Nair, R. M. Philip, G. Anilkumar, *Org. Biomol. Chem.* **2021**, *19*, 4228–4242.

[39] A. Gualandi, F. Calogero, D. Corbisiero, E. Pinosa, P. G. Cozzi, *Asian J. Org. Chem.* **2024**, *13*, e202300574.

[40] O. Gutierrez, J. C. Tellis, D. N. Primer, G. A. Molander, M. C. Kozlowski, *J. Am. Chem. Soc.* **2015**, *137*, 4896–4899.

[41] F. Lukas, M. T. Findlay, M. Fillols, J. Templ, E. Savino, B. Martin, S. Allmendinger, M. Furegati, T. Noël, *Angew. Chem. Int. Ed.* **2024**, *63*, e202405902.

[42] J. A. Milligan, J. P. Phelan, S. O. Badir, G. A. Molander, *Angew. Chem. Int. Ed.* **2019**, *58*, 6152–6163.

[43] J. Kim, S. Müller, T. Ritter, *Angew. Chem. Int. Ed.* **2023**, *62*, e202309498.

[44] L. Huang, M. Rueping, *Angew. Chem. Int. Ed.* **2018**, *130*, 10490–10494.

[45] A. Pulcinella, P. C. Tiwari, A. Luridiana, K. Yamazaki, D. Mazzarella, A. K. Sadhoe, A. I. Alfano, E. H. Tiekink, T. A. Hamlin, T. Noël, *Angew. Chem. Int. Ed.* **2024**, *64,* e202413846.

[46] A. Luridiana, D. Mazzarella, L. Capaldo, J. A. Rincón, P. García-Losada, C. Mateos, M. O. Frederick, M. Nuño, W. Jan Buma, T. Noël, *ACS Catal.* **2022**, *12*, 11216–11225.

[47] E. M. Dauncey, S. U. Dighe, J. J. Douglas, D. Leonori, *Chem. Sci.* **2019**, *10*, 7728–7733.

[48] R. Chen, N. E. Intermaggio, J. Xie, J. A. Rossi-Ashton, C. A. Gould, R. T. Martin, J. Alcázar, D. W. C MacMillan, *Science* **2024**, *383*, 1350–1357.

[49] J. Z. Wang, E. Mao, J. A. Nguyen, W. L. Lyon, D. W. C. MacMillan, *J. Am. Chem. Soc.* **2024**, *146*, 15693–15700.

[50] J. Z. Wang, W. L. Lyon, D. W. C. MacMillan, *Nature* **2024**, *628*, 104–109.

[51] S. Dongbang, A. G. Doyle, *J. Am. Chem. Soc.* **2022**, *144*, 20067–20077.

[52] S. H. Lau, M. A. Borden, T. J. Steiman, L. S. Wang, M. Parasram, A. G. Doyle, *J. Am. Chem. Soc.* **2021**, *143*, 15873–15881.

[53] T. Kim, S. J. McCarver, C. Lee, D. W. C. MacMillan, *Angew. Chem. Int. Ed.* **2018**, *57*, 3488–3492.

[54] M. S. Oderinde, N. H. Jones, A. Juneau, M. Frenette, B. Aquila, S. Tentarelli, D. W. Robbins, J. W. Johannes, *Angew. Chem. Int. Ed.* **2016**, *55*, 13219–13223.

[55] E. B. Corcoran, M. T. Pirnot, S. Lin, S. D. Dreher, D. A. Dirocco, I. W. Davies, S. L. Buchwald, D. W. C. MacMillan, *Science* **2016**, *353*, 279–283.

[56] M. Jouffroy, C. B. Kelly, G. A. Molander, *Org. Lett.* **2016**, *18*, 876–879.

[57] H. Yue, C. Zhu, M. Rueping, *Angew. Chem. Int. Ed.* **2018**, *57*, 1371–1375.

[58] J. Düker, M. Philipp, T. Lentner, J. A. Cadge, J. E. A. Lavarda, R. M. Gschwind, M. S. Sigman, I. Ghosh, B. König, *ACS Catal.* **2024**, 817–827.

[59] I. Ghosh, N. Shlapakov, T. A. Karl, J. Düker, M. Nikitin, J. V. Burykina, V. P. Ananikov, B. König, *Nature* **2023**, *619*, 87–93.

[60] 4-(trifluoromethyl)picolinamidine has been used as a ligand in on-DNA C-N coupling reactions: D. K. Kölmel, J. Meng, M. H. Tsai, J. Que, R. P. Loach, T. Knauber, J. Wan, M. E. Flanagan, *ACS Comb. Sci.* **2019**, *21*, 588–597.

[61] L. Y. Vázquez-Amaya, G. A. Coppola, E. V. Van der Eycken, U. K. Sharma, *J. Flow Chem.* **2024**, *14*, 257–279.

[62] L. Capaldo, Z. Wen, T. Noël, *Chem. Sci.* **2023**, *14*, 4230–4247.

[63] F. Darvas, G. Dormán, V. Hessel and S. V. Ley, *Volume 1, Flow Chemistry - Fundamentals*, De Gruyter, **2021**.

[64] F. Darvas, G. Dormán, V. Hessel and S. V. Ley, *Volume 2, Flow Chemistry - applications*, De Gruyter, **2021**.

[65] C. Sambiagio, T. Noël, *Trends Chem.* **2020**, *2*, 92–106.

[66] T. H. Rehm, *Chem. Eur. J.* **2020**, *26*, 16952–16974.

[67] S. A. Weissman, N. G. Anderson, *Org. Process Res. Dev.* **2015**, *19*, 1605–1633.

[68] C. J. Taylor, A. Baker, M. R. Chapman, W. R. Reynolds, K. E. Jolley, G. Clemens, G. E. Smith, A. J. Blacker, T. W. Chamberlain, S. D. R. Christie, B. A. Taylor, R. A. Bourne, *J. Flow Chem.* **2021**, *11*, 75–86.

[69] "MODDE® - Design of Experiments Software _ Sartorius," can be found under https://www.sartorius.com/en/products/process-analytical-technology/data-analytics-software/doe-software/modde, **2024.**

[70] P. M. Murray, F. Bellany, L. Benhamou, D. K. Bučar, A. B. Tabor, T. D. Sheppard, *Org. Biomol. Chem.* **2016**, *14*, 2373–2384.

[71] K. J. Liang, O. R. Taylor, A. L. López, R. J. Woo, A. Bahamonde, *Chem. Eur. J.* **2024**, *30,* e202402524.

[72] L. Geniller, M. Taillefer, F. Jaroschik, A. Prieto, *Adv. Synth. Catal.* **2022**, *364*, 4249–4254.

[73] T. Q. Chen, D. W. C. MacMillan, *Angew. Chem. Int. Ed.* **2019**, *58*, 14584-14588.

[74] Didier Candau (L'Oreal SA), **2006**, US_2006177394_A1.

[75] N. A. Till, PhD thesis, Princeton University, **2021**.

[76] S. Hattori, S. Hirata, K. Shinozaki, *J. Phys. Chem. B* **2021**, *125*, 9260–9267.

[77] H. Huang, W. Guo, W. Wu, C. J. Li, H. Jiang, *Org. Lett.* **2015**, *17*, 2894–2897.

[78] R. D. Bradley, B. D. McManus, J. G. Yam, V. Carta, A. Bahamonde, *Angew. Chem. Int. Ed.* **2023**, *62*, e202310753.

[79] B. D. McManus, L. C. Hung, O. R. Taylor, P. Q. Nguyen, A. L. Cedeño, K. Arriola, R. D. Bradley, P. J. Saucedo, R. J. Hannan, Y. A. Luna, P. Farias, A. Bahamonde, *J. Am. Chem. Soc.* **2024**, *146*, 32135–32146.

[80] N. A. Till, L. Tian, Z. Dong, G. D. Scholes, D. W. C. MacMillan, *J. Am. Chem. Soc.* **2020**, *142*, 15830–15841.

[81] R. Sun, Y. Qin, D. G. Nocera, *Angew. Chem. Int. Ed.* **2020**, *59*, 9527–9533.

[82] R. Escobar, J. Johannes, *Chem. Eur. J.* **2020**, *26*, 5168–5173.